582 **RESEARCH PAPER** SEPTEMBER, 582–587 JOURNAL OF CHEMICAL RESEARCH 2009

Synthesis, spectroscopic investigation and biological activity of metal(II) complexes with N_2O_4 ligands

Abdou Saad El-Tabl[b]*, Winfried Plass[a], Axel Buchholz[a] and Mohamad M.E. Shakdofa[c]

[a]*Chemistry Department, Friedrich-Schiller Universität, Jena, Germany*

[b]*Chemistry Department, Faculty of Science, Menoufia University, Shebin El-Kom, Egypt*

[c]*Inorganic Chemistry Department, National Research Centre, P.O. 12622 Dokki, Cairo, Egypt*

A new series of Mn(II), Ni(II), Co(II) and Cu(II) complexes derived from diacetylmonoxime and 2-, 4- and 6-aminobenzoic acids have been prepared and characterised by elemental and thermal analyses (DTA, DTG and TG) as well as ^{1}H and ^{13}C NMR, IR, UV-Vis., Mass and ESR spectra, magnetic susceptibility and conductance measurements. The IR spectral data show that the ligands behave as mono- or di-basic, bis-, tri-, or tetradentate-chelates towards the metal ion. The stability of the complexes is achieved *via* intra- and inter-molecular hydrogen bonding of the OH-group with the oximato-oxygen atom or oxygen atom of a carboxylic group, giving polymeric networks in the solid state. Molar conductances in DMF solution indicate that the complexes are non-electrolytes. The ESR spectra of solid complexes $[Co(HL^1)_2].2H_2O$ **(4)**, $[Mn(HL^1)_2].H_2O$ **(5)**, $[Mn(HL^2)_2(H_2O)_2].H_2O$ **(10)**, $[Cu_2(HL^3)_2(OAc)_2(H_2O)_4]$ **(12)** and $[(Mn)_3(L^3)_2(OAc)_2(H_2O)_6].4H_2O$ **(15)** at room temperature and 77 K, are isotropic, however, the copper(II) complexes $[Cu(HL^1)(OAc)(H_2O)_2\}_2]$ **(2)** and $[Cu(HL^2)_2(H_2O)_2].H_2O$ **(7)** are non-axial and axial ($d_{x2\text{-}y2}$) respectively with covalent bond character. The metal complexes exhibit greater inhibitory effects than tetracycline (bacteria) and amphotricen (fungi).

Keywords: spectral and magnetic measurements, biological activity, metal(II) complexes, N_2O_4 ligands

Much attention has been given recently to the design of polymeric structures with interesting structural and magnetic properties. The focus has been on understanding the ability of bridging polytopic ligands to mediate coupling in bridged ligand–metal systems, since exchange coupling is an important phenomenon, especially in multi-metal containing proteins.[1-3] Therefore, several polymetallic systems have been studied in order to comprehend fundamental electronic process in metallobiosites, because of the structural similarity between polymeric compounds and natural materials, as well as the kinds of functions exhibited by polymeric compounds. Di- and tri-nuclear copper(II) complexes with extended bridging systems such as oxalate,[4,5] oximate,[6] phenolate[6-8] and carbonate[9] have been reported to mediate strong exchange coupling between paramagnetic centres. Among multi-atom bridging ligands, carboxylate has been extensively studied. The carboxylic group is known to exhibit different types of bridging conformations. Numerous examples exist of structurally characterised copper(II) complexes involving the triatomic bridging mode, but only a few of them have been studied magnetically.[10,11] Thus, earlier reports have included acetylacetonate–carboxylate,[12] oxinate–carboxylate,[13] oximate–carboxylate[14] and keteonamine–carboxylate complexes.[15] Interest in such oxime–carboxylate complexes lies in their ability as polymers, catalysts, fungicides and bactericides.[16,17] We now report the syntheses, structures, spectroscopy, magnetic properties and biological activity of new copper(II), nickel(II), cobalt(II) and manganese(II) complexes derived from diacetylmonoxime with 2-, 4-, and 6-aminobenzoic acid.

Experimental

Reagent grade chemicals were used. Diacetylmonoxime was prepared by a published method.[18] Carbon, hydrogen and nitrogen contents were determined at the Institut für Organische und Makromolekulare Chemie, Friedrich-Schiller-University, Jena, using LECO CHN/932 and VARIO El III elemental analysers. Standard methods were used to determine the metal(II) ion content. All metal(II) complexes were dried in air. The IR spectra were recorded on a Bruker IFS 55/Equinox spectrometer on complexes prepared as KBr pellets. Electronic spectra were recorded on a Varian Cary 5000 UV/VIS/NIR spectrophotometer. The conductance of 10^{-3} M solutions of the complexes in DMF was measured at 25 °C with a Bibby Conductimeter type MCl. The magnetic susceptibilities were measured by the Gouy method on polycrystalline samples. ^{1}H and ^{13}C NMR spectra were recorded on Bruker Avance 200 and 400 MHZ spectrometers. Mass spectrometry was conducted on a Mat95XL Finnigan instrument, using electron spray ionisation, negative and positive mode. Thermal analyses were carried out using a NETZSCH STA 409PC/PG instrument and the samples were placed in a heating block with a heating rate of 5 K/min under a nitrogen atmosphere. All ESR measurements on solid complexes at 300 K and 77 K were made using a Bruker ESP 300 E spectrometer, using X-band (9 GHZ). DPPH was used as an external standard.

Preparation of the ligands $[H_2L^1].H_2O$ **(1)**, $[H_2L^2]$ **(6)** and $[H_2L^3].\frac{1}{4}H_2O$ **(11)**: An ethanolic solution (50 mL) of 2-, 4- or 6-aminobenzoic acid (10,6 g, 0,078 mol) was added dropwise to an ethanolic solution (50 mL) of diacetylmonoxime (10,0 g, 0,078 mol) and the mixture was boiled under reflux for 1 h, then left to cool at room temperature. The precipitated ligand was filtered off, washed with warm ethanol, dried and recrystallised from ethanol.

Preparation of metal complexes

Copper(II) complexes **(2)**, **(7)** *and* **(12):** A filtered ethanolic solution (50 mL) of $Cu(OAc)_2.H_2O$ (4.1 g, 0.02 mol) was added to an ethanolic solution (50 mL) of the ligand **(1)**, **(6)** or **(11)** (5.0 g, 0.02 mol). The mixture was refluxed with stirring for 3 h. The complexes which formed were filtered off, washed several times with warm ethanol and dried in air.

Nickel(II), cobalt(II) and manganese(II) complexes **(3–5)**, **(8–10)**, **(13–15):** Using a 1 : 1 molar ratio of a suitable ligand and the corresponding metal acetate, the reaction was carried out as described above. The precipitated complexes were filtered off, washed with ethanol and dried in air.

Antibacterial and antifungal screening

The antibacterial and antifungal activities of the ligands and their complexes were tested using the disc diffusion method[19] against gram positive bacteria *(Bacillus Subtile)* and gram negative bacteria (*E. Coli)*) and fungi *(Aspergillus Niger)*. Nutrient agar medium for bacteria was prepared using peptone, beef extract, NaCl, agar-agar and distilled water, while Chapek's Dox medium for fungi was prepared using yeast extract, sucrose, $NaNO_3$, agar, KCl, KH_2PO_4, $MgSO_4.7H_2O$ and a trace of $FeCl_3.6H_2O$. The test compounds in measured quantities were dissolved in DMSO solution to give a concentration of 20 mg mL^{-1} of compounds. Twenty five millilitres of nutrient agar medium was poured into each Petri plate. After solidification, 0.1 mL of test bacteria was then spread over the medium using a sterile bent loop rod. Discs were cut by a sterilised cork borer and then taken by sterilised needle The resulted pits are sites for the tested compounds. The plates of bacteria were incubated at 37 °C for 48–72 h while the plates of fungi were incubated at 30 °C for 48–72 h and then any clear zones present were measured. The DMSO solution served as

---

* Correspondent. E-mail:asaeltabl@yahoo.com

a control, and tetracyclin was used as a bacterial standard drug while amphotricen was used as a fungal standard drug. All determinations were made in duplicate for each of the compounds. An average of two independent readings for each compounds was recorded.

Results and discussion

Our interests in this area are in the use of multifunctional ligands whose donor atoms are located on a rigid phenyl group. For this purpose, we use Schiff-bases derived from aromatic amino acids and carbonyl oxime compounds as shown in **(1), (6)** and **(11)**, for the following reasons. First they contain carboxylate and oxime functionalities, which are known to behave differently towards metal centres because of differences in their hard-soft donor characteristics. Secondly, by choosing the second substituent's position (namely, 2, 4 or 6; *i.e.* 60, 120 or 180° between the functional groups) one can easily vary the resultant polymeric organisation. The metal complexes are best prepared by mixing a 1:1 molar ratio of the ligand with a metal acetate under reflux conditions in ethanolic solution. All the complexes are intensely coloured, stable at room temperature, non hygroscopic, insoluble in water and partly soluble in common organic solvents such as $CHCl_3$ but soluble in DMF and DMSO. The analytical and physical data (Table 1) and spectral data (Tables 2 and 3) are consistent with the proposed structures (Fig. 1). To date, no diffractable crystals could be obtained.

Diacetylmonoxime reacts with 2-, 4-, and 6-aminobenzoic acids (1 : 1, molar ratio) in ethanol to give new Schiff-bases, which react with metal(II) acetates in molar ratios (1L:1M), (2L:1M) or (1L:2M), in ethanol, leading to the formation of different complexes, depending on the position of the carboxylic group. The reaction of 2-, 4-, and 6-aminobenzoic acids, diacetylmonoxime and metal(II) acetate (1 : 1,: 1 molar ratio) in ethanol led to the formation of similar complexes.

^{1}H- and ^{13}C NMR spectra

The ^{1}H NMR spectra of the ligands **(1), (6)** and **(11)** in deuteriated DMSO show the absence of amine groups belonging to the starting material and the N–OH chemical shift appears at 12.95 for **(1)** and 12.42 ppm for **(11)**, but in **(6)** no signal for NOH was observed, indicated that diacetylmonoxime had condensed with the aminobenzoic acid. The aromatic protons appear as multiplets in the 6.48–8.0 ppm range and the methyl protons in the 2.17–2.33 ppm range.[20,21] The C^{13} NMR spectral data were obtained in deuteriated DMSO. For **(1),** the peaks at 200.2, 194.9 and 169.6 ppm correspond to acetyl, carboxylic and oxime groups respectively and the peaks in the 133.8–109.7 ppm range are due to the aromatic carbon atoms.[22] Moreover, the peaks in the 38.9–48.7 ppm range are due to the methyl group. Other carbon resonances are doublets, indicating that the ligand has *cis–trans* isomerism.[4] Ligand **(6)** shows the carboxylic carbon atom at 168.3, C=NOH at 149.3 ppm and the aromatic carbon atoms in the 131.8–114.9 ppm range, whereas the methyl carbon atoms appear in the 40.6–39.3 ppm range. Ligand **(11)** shows the carboxylic carbon atom at 200.6 and C=OH at 195.3 ppm, the aromatic carbon atoms in the 168.0–113.0 ppm range, and the methyl carbon atoms at 40.6 ppm.

IR spectra

Important spectral bands of the ligands and their metal complexes are presented in Table 2. The IR spectra of the metal complexes have been interpreted by comparing the spectra with those of the free ligands. The ligands spectra show two υ(OH) bands, indicating the presence of two types of hydrogen bonded oxime and carboxylic groups which could be intra- and inter-molecularly hydrogen bonded to the basic imino-nitrogen atom or to the C=O of a carboxylic group. Thus, the higher frequency band in the range 3600–3000 cm^{-1} is associated with a weaker hydrogen bonding compared with the lower frequency

Table 1 Elemental analyses and physical properties of the ligands and their metal complexes

No.	Molecular formula	Colour	Yield /%	M.P /°C	Ω mol^{-1} /cm^2	μ_{eff} BM	Found (Calcd)/%			
							C	H	N	M
1	$[H_2L^1]_2.2H_2O$ $[C_{24}H_{28}N_4O_{10}]$	Yellow	82	>300	0.61	–	54.5(54.2)	5.0(5.3)	10.5(10.2)	–
2	$[\{Cu(HL^1)\ (OAc)(H_2O)_2\}_2]$ $[C_{28}H_{36}N_4O_{16}Cu_2]$	Pale green	72	>300	2.31	1.68	41.7(41.4)	4.1(4.4)	7.3(7.0)	15.3(15.8)
3	$[\{Ni(HL^1)(OAc)\}_2].H_2O$ $[C_{28}H_{30}N_4O_{13}Ni_2]$	Brown	62	>300	3.27	2.93	45.3(45.0)	4.0(4.0)	8.1(7.5)	16.5(15.82)
4	$[Co\ (HL^1)_2].2H_2O$ $[C_{24}H_{26}N_4O_{10}Co]$	Yellowish brown	58	>300	1.82	4.1	48.5(48.9)	4.3(4.4)	9.8(9.5)	9.8(11.1)
5	$[Mn\ (HL^1)_2].H_2O$ $[C_{24}H_{24}N_4O_9Mn]$	Yellow	68	>300	2.26	4.98	50.0(50.7)	4.1(4.2)	9.2(9.8)	8.9(9.7)
6	$[H_2L^2]_2$ $[C_{24}H_{24}N_4O_8]$	Brownish yellow	70	>300	0.4	–	58.0(58.1)	5.0(4.8)	11.0(11.3)	–
7	$[Cu\ (HL^2)_2(H_2O)_2].H_2O$ $[C_{24}H_{28}N_4O_{11}Cu]$	Deep green	85	>300	5.32	1.75	48.0(47.3)	4.4(4.3)	9.0(9.2)	10.1(10.5)
8	$[Ni\ (HL^2)_2(H_2O)_2].3H_2O$ $[C_{24}H_{32}N_4O_{13}Ni]$	Yellowish brown	75	>300	3.8	3.32	44.9(44.6)	4.6(4.6)	8.4(8.7)	8.9(9.13)
9	$[Co(HL^2)_2(H_2O)_2].H_2O$ $[C_{24}H_{28}N_4O_{11}Co]$	Pale brown	70	>300	4.9	4.23	48.0(47.6)	4.4(4.3)	9.4(9.3)	9.5(9.7)
10	$[Mn(HL^2)_2(H_2O)_2].H_2O$ $[C_{24}H_{28}N_4O_{11}Mn]$	Brown	65	>300	6.2	5.12	48.0(47.9)	4.3(4.3)	9.0(9.3)	9(9.1)
11	$[(H_2L^3)_2].0.5H_2O$ $[C_{24}H_{25}N_4O_9]$	Yellow	73	>300	0.4	–	57.0(57.0)	5.4(5.0)	11.0(11.1)	–
12	$[Cu(HL^3)(OAc)(H_2O)].H_2O$ $[C_{14}H_{18}N_2O_8Cu]$	Deep green	70	>300	0.7	82	41.1(41.4)	4.1(4.4)	6.8(6.9)	15.2(15.7)
13	$[Ni(HL^3)(OAc)(H_2O)_3].3H_2O$ $[C_{14}H_{26}N_2O_{12}Ni$	Brown	62	>300	2.7	3.32	35.4(35.5)	5.4(4.6)	5.7(5.9)	12.3(12.5)
14	$[(Co)_3\ (HL^3)_2(OAc)_2(H_2O)_6].H_2O$ $[C_{14}H_{24}N_2O_{11}Co]$	Brown	65	›300	2.3	4.43	36.2(36.9)	5.2(5.3)	6.0(6.1)	13.0(12.9)
15	$[(Mn)_3\ (L^3)_2(OAc)_2(H_2O)_6].4H_2O$ $[C_{14}H_{26}N_2O_{12}Mn]$	Brown	58	>300	5.2	4.93	35.6(35.8)	6.0(5.97)	5.8(5.91)	12.1(11.73)

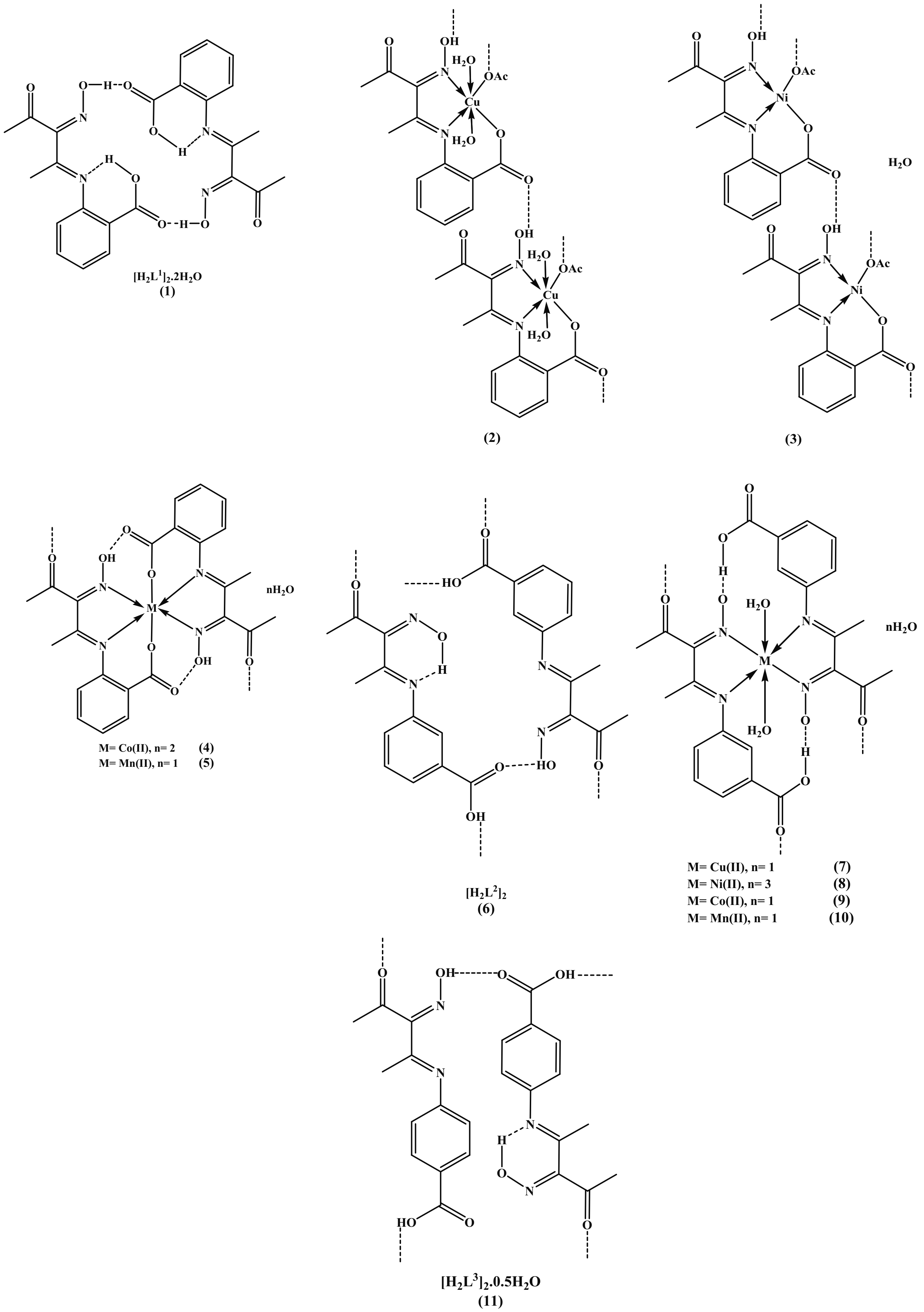

Fig.1 Structural representation of the ligands and their metal complexes.

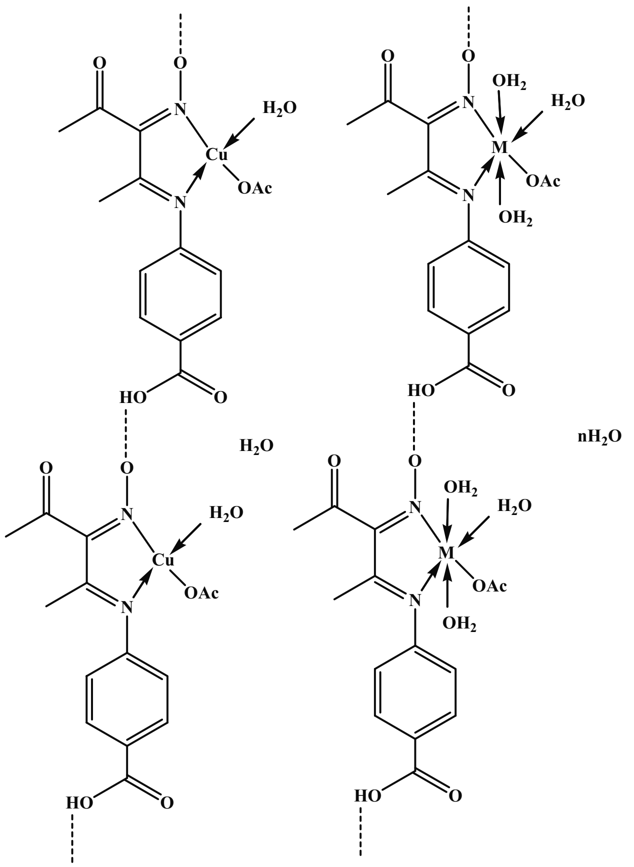

(12)

M= Ni(II), n= 3 (13)
M= Co(II), n= 2 (14)
M= Mn(II), n= 3 (15)

Fig.1 *Continued*

band in the range 3100–2350 cm^{-1} of the relatively stronger hydrogen bonding. The $\upsilon(C{=}O_{Acetyl})$ and $\upsilon(C{=}O_{Carboxylic})$ of the ligands appear in the 1722–1687 and 1670–1653 cm^{-1} ranges respectively.[15,23] The (C=N) vibrations (imine and oxime) are located in the 1628–1614 and 1603–1589 cm^{-1} ranges.[24] However, the band in the 1585–1564 cm^{-1} range is assigned to $\upsilon(C{=}C_{Ar})$. The splitting of the υ(N–O) vibration of the 2-, 4-, and 6- ligands into two bands appearing at 1066, 1025; 1016, 1000 and 998, 985 cm^{-1} respectively is consistent with the presence of non-equivalent hydrogen bonding. The IR spectra of the metal complexes show that the υ(C=N) vibrations (imine and oxime) undergo a shift to lower frequency by (9–38 cm^{-1}) (imine), except complexes **(7)** and **(9)**, (2–23 cm^{-1}) (oxime), except complexes **(8)** and **(12)**. This is indicative of nitrogen coordination of the azomethine and oxime groups to the metal ion.[22,23,25,26] The $\upsilon(C{=}O_{acetyl})$ of the complexes appears in the 1720–1665 cm^{-1} range. This vibration is located in the region of non-coordinated carbonyl groups attached to a five-membered chelate ring.[23] The $\upsilon(C{=}O_{carboxylic})$ band appears in the 1655–1614 cm^{-1} range, except complexes **(7)** and **(9)**. The shift of this band indicates the formation of H-bonding (O–H–O type) in these complexes, which probably stabilises the proposed structures (Fig. 1). A new band in the 1215–1155 cm^{-1} range corresponds to N-coordination of the oximato-group.[27,28] The strong broad band in the 3650–3215 cm^{-1} range, confirms the presence of water molecules in all complexes except **(3).**[40,41] Also, the complexes show $\upsilon(C = C_{Ar})$ in the 1585–1540 cm^{-1} range. Complexes **(2), (3)** and **(10)** show bands in the 1553–1515 and 1452–1409 cm^{-1} ranges, assigned to the asymmetric and symmetric stretches of the (COO) group with a Δυ value $[\upsilon_{sym}(CO^-_2)_a - \upsilon_{sym}(CO^-_2)]$ in the range of 117–101 cm^{-1}, which is consistent with the monodentate coordination of carboxylate oxygen.[23,29,30] The bonding of metal(II) ions to the ligand through the nitrogen and oxygen atoms is further supported by the presence of new bands in the 668–635 and 600–545 cm^{-1} ranges, due to υ(M–O) and υ(M–N) respectively.[31]

Conductivity

The molar conductances of the complexes in DMF solutions lie in the 0.4–6.2 $\Omega^{-1}cm^2mol^{-1}$ range (Table 1), indicating their non-electrolytic nature.[31,32]

Electronic spectra

The electronic spectra of the ligands and their metal(II) complexes (nujol mulls and DMF solutions) are summarised in Table 3. The spectra of the ligands **(1), (6)** and **(11)** in nujol mulls show peaks at 260, 250 and 230 nm; 370, 335 and 315 nm respectively. However, in DMF they give one peak only at 350 nm (Є = 25 × 10^{-3} mol^{-1} cm^{-1}) **(1)**, 315 nm (23 × 10^{-3} mol^{-1} cm^{-1}) **(6)** and 288 nm (Є = 22 × 10^{-3} mol^{-1} cm^{-1}) **(11)**, which is assigned to $\pi\rightarrow\pi^*$ and $n\rightarrow\pi^*$ transitions in the ligands.[24,33] In nujol mulls, the spectra of the copper(II) complexes **(2)** and **(7)** show bands at 290, 410, 590 and 650; 293, 475, 560 and 670; 295, 460, 570 and 650 nm respectively. However, in DMF, bands are observed at 270, 405, 495 and 610; 275, 310, 420, 515 and 625; 290, 425, 530 and 602 nm respectively. The first band is assigned to an intraligand transition and the other bands correspond to $^2B_{1g}\rightarrow{}^2E_g$, $^2B_{1g}\rightarrow{}^2B_{2g}$ and $^2B_{1g}\rightarrow{}^2A_{1g}$, transitions of the copper(II) ion in a tetragonally-elongated octahedron.[34,35] However, complex **(12)** shows, in nujol mull, bands at 295, 460 and 570 nm and in DMF, at 305, 425 and 530 nm. The first band is due to an intraligand transition, however the other two bands are assigned to $^2B_{1g}\rightarrow{}^2B_{2g}$ and $^2B_{1g}\rightarrow{}^2A_{1g}$, transitions of a square planar copper(II) ion.[25] In nujol mulls, the nickel(II) complexes **(8)** and **(13)** exhibit bands at 290, 380, 410 and 650; 300, 410, 590 and 650 nm. However, in DMF, the bands appear at 285, 365, 407 and 585; 260, 365, 400 and 605 nm respectively. The first two are within the ligand and the other bands are assigned to $^3A_{2g}\rightarrow{}^3T_{1g}$ (υ_2) and $^3A_{2g}\rightarrow{}^3T_{2g}$ (υ_1) transitions in an octahedral structure.[23,36] The υ_2/υ_1 values are 1.54 and 1.59 which lie in the range expected for octahedral geometry.[23] However, complex **(3)** shows bands in nujol mull at 292, 365, 425 and 615 but in DMF, the bands appear at 267, 320, 420 and 610 nm. The first two are within the ligand and the other bands are assigned to $^3T_1\rightarrow{}^3T_1$ (P) and $^3T_1\rightarrow{}^3T_2$ transitions of a tetrahedral or pseudooctahedral structure.[37] The cobalt(II) complexes **(4), (9)** and **(14)** give bands in nujol mulls located at 310, 375, 460 and 665; 285, 350, 495 and 625; 285, 350, 520 and 625 nm. However, in DMF the bands appear at 297, 350, 425 and 657; 275, 350, 510 and 610; 280, 360, 485 and 595 nm. The first two bands are within the ligand and the other bands correspond to $^4T_{1g}(F)\rightarrow{}^4A_{2g}(F)$ and $^4T_{1g}(F)\rightarrow{}^4T_{1g}(P)$ transitions respectively characteristic of octahedral geometry.[38,39] The spectra of manganese(II) complexes **(5), (10)** and **(15)** in nujol mull, show bands at 275, 330, 450, 580 and 610; 295, 335, 450, 550 and 600; 255, 295, 450, 590 and 640 nm. However, in DMF the bands are observed at 250, 310, 420, 505 and 575; 285, 320, 415, 505 and 570; 275, 310, 480, 540 and 603 nm. The first two bands are within the ligand and the other bands are assignable to $^6A_{1g}\rightarrow{}^4T_{2g}$ (D), $^6A_{1g}\rightarrow{}^4T_{2g}$(G) and $^6A_{1g}\rightarrow{}^4T_{1g}$, transitions respectively indicating an octahedral structure.[31,40] The positions of the peaks observed for the nujol mull spectra are not identical with those observed from the DMF solution. Accordingly, it is suggested that, all these observed bands are related to charge transfer transitions generated from intermolecular hydrogen bonding.

Magnetic moments

Room temperature magnetic moments of the complexes **(2)–(5), (7)–(10)** and **(12)–(15)** are presented in Table 1. Copper(II) complexes **(2), (7)** and **(12)** show values 1.68, 1.75 and 1.82 BM, indicating octahedral or square planar geometry around the copper(II) ion.[41] Nickel(II) complexes **(3), (8)** and **(13)** show values 2.93, 3.32 and 3.32 BM, indicating tetrahedral or octahedral nickel(II) complexes.[32,42,43] Cobalt(II) complexes **(4), (9)** and **(14)** show values 4.1, 4.23 and 4.43 BM, indicating high spin octahedral cobalt(II) complexes.[44] The magnetic moment values for manganese(II) complexes **(5), (10)** and **(15)** are 4.98, 5.12 and 4.793 BM, suggesting octahedral geometry around the manganese(II) ions.[45]

ESR spectra

The ESR spectra of solid copper(II) complexes **(2), (7)** and **(12)** at room and liquid nitrogen temperatures are characteristic of a d^9 system with a $d_{(x2\text{-}y2)}$ ground state, which is most common for copper(II) complexes.[46,47] Complex **(2)** at RT shows non-axial type symmetry with three g-values $g_1 = 2.2521$, $g_2 = 2.1135$ and $g_3 = 2.075$ and $(g_2 - g_3)/(g_1 - g_2) < 1$ (= 0.28), indicating a $d_{(x2-y2)}$ ground state with covalent bond character.[48] The shift of the signals to slightly lower values at 77 K, $g_1 = 2.2419$, $g_2 = 2.1129$ and $g_3 = 2.0637$ indicates a stronger metal-ligand bonding, consistent with octahedral distortion present at room temperature.[48] However, at RT complex **(7)** shows an axial type symmetry with $g_{\parallel} = 2.282$, $g_{\perp} = 2.068$ and $g_{iso} = 2.14$. The $g_{\parallel} > g_{\perp}$ is commensurate with a distorted octahedral complex.[27,49]

Table 2 IR spectra (assignments) of the ligands and their metal complexes

No.	$\upsilon(H_2O$/H-bonding)	$\upsilon(OH)_{Carb./Oxime}$	$\upsilon(C=O)_{acetyl}$	$\upsilon(C=O)_{carb.}$	$\upsilon(C=N)_{imine}$	$\upsilon(C=N)_{Oxime}$	$\upsilon(C=C)_{Ar}$	υ(OAc)	υ(Oxime)	υ(M–O)	υ(M–N)
1	3560–3000 2990–2350	3473 3373	1722	1670	1617	1589	1564	–	1000 1025	–	–
2	3575–3300 3295–2900	– 3276	1686	1630	1606	1586	1572	1553 1452	1168 1113	650	550
3	3600–3350 3257–2920	– 3305	1698	1615	1603	1589	1568	1542 1426	1190 1175	635	558
4	3650–3368 3290–2890	– 3308	1670	1614	1591	1580	1540	– –	1182 1039	660	583
5	3600–3320 3300–2875	– 3305	1665	1616	1589	1575	1542	– –	1190 1088	635	573
6	3600–3080 3070–2370	3358 3100	1690	1656	1614	1600	1585	–	1066 998	–	–
7	3629–3420 3400–2400	3250 3134	1720	1685	1629	1598	1586	1567 1458	1067 1150	668	590 545
8	3600–3267 3260–2470	3255	1700	1645	1628	1605	1562	– –	1160	665	595
9	3643–3360 3350–2420	3235	1715	1668	1605	1586	1566	– –	1187	635	552
10	3635–3330 3300–2500	3358 3250	1720	1657	1589	1578	1556	1546 1415	1020 1215	668	546
11	3530–3170 3100–2400	3461 3364	1687	1657 1653	1628	1603	1574	– –	985 1016	–	–
12	3600–3329 3560–2850	3252, 3125 –	1700	1642	1624	1607	1571 1434	1557 1142	1195	658	572
13	3650–3250 3425–2800	– –	1672	1650	1590	1585	1570	1551 1450	1176 1116	650	590
14	3580–3215 3369–2750	– –	1680	1653 1643	1601	1580	1559	1540 1423	1177 1122	660	600
15	3660–3290 3430–2885	– –	1681	1645	1602	1595	1557	1551 1450	1174 1150	643	585

Table 3 Electronic spectra of the ligands and their metal complexes

No.	λ_{max}/nm in DMF	λ_{max}/nm in Nujol mull
1	350 $\epsilon = 25 \times 10^{-3}$ mol^{-1} cm^2	370, 260
2	610, 495, 405, 270	650, 590, 410, 290
3	610, 420, 320, 267	615, 425, 365, 292
4	657, 425, 350, 297	665, 460, 375, 310
5	575, 505, 420, 310, 250	610,580, 450, 330, 275
6	315 $\epsilon = 23 \times 10^{-3}$ mol^{-1} cm^2	335, 250
7	625, 515, 420, 310	760, 560, 475, 295
8	585, 407, 365, 285	650, 410, 380, 290
9	610, 510, 350, 275	625, 495, 350, 285
10	570, 490, 370, 320	600, 550, 450, 335, 295
11	288 $\epsilon = 22 \times 10^{-3}$ mol^{-1} cm^2	315, 230
12	530, 425, 305	570, 460, 295
13	605, 400, 365, 260	650, 590, 410, 300
14	595, 485, 370, 280	625, 520, 350, 285
15	603, 540, 480, 310, 275	640, 590, 450, 295, 255

The spectrum at 77 K is almost identical to that at RT indicating that the geometry of the complex is not changed on lowering the temperature. The $g_{||}$ value indicate a covalent bond character.[47] Also the g-values of complex **(7)** shows G = 4.15, indicating tetragonal axes present in this complex.[50] For copper(II) complexes with $^2B_{1g}$ ground state ($g_{||} > g_{\perp}$), the orbital reduction factors $K_{||}$, $K_{\perp}$ and K are used as a measure of covalency.[51] For an ionic environment K = 1 and for a covalent environment K < 1. In the present complex $K_{||} = 0.867$, $K_{\perp} = 0.945$ and K = 0.92, these values show considerable covalent bonding character. Complex **(12)** shows isotropic values with $g_{iso}(RT) = 2.114$ and $g_{iso}(77\ K) = 2.113$, confirmed the square planar structure[46,47] The cobalt complex **(4)** shows an isotropic value with $g_{iso} = 1.995$ at RT and 77 K indicating an octahedral structure.[48] However, the manganese complexes **(5)**, **(10)** and **(15)** show isotropic type spectra with $g_{iso} = 2.021$, 2.017 and 2.014 respectively, indicating octahedral geometry around the manganese(II) ion.[48]

ESI-MS studies

The molecular composition of the ligands **(1)**, **(6)** and **(11)** and their metal complexes **(7)**, **(8)**, **(9)**, **(12)**, **(13)** and **(14)** has been investigated by ESI mass spectral analysis. ESI mass spectra of the ligands **(1)**, **(6)** and **(11)** were recorded in MeOH. However, for complexes **(7)**, **(8)**, **(9)**, **(12)**, **(13)** and **(14)** the spectra were recorded in a 1 : 1 solvent mixture of MeOH and DMSO, because of a solubility problem. As indicated by the observed masses in both positive and negative ions, the spectra of the ligands are found to exist in solution as tetrameric **(1)** and **(11)** and a monomeric species **(6)**. The positive ion ESI mass observed for **(1)**, shows the presence of $[C_{14}H_{12}N_3O_5]^+$ (302, 100) with a less intense peak found for $[C_{22}H_{13}N_4O_5]^+$. However, compound **(6)** shows the presence of $[C_9H_8O_2N]^+$ (162, 100) and additional less intense peaks for $[C_7H_5O_2]^+$ (121, 12), $[C_2H_3O]^+$ (43, 40) and $[C_{10}H_9O_3N_2]^+$ (205, 25) and compound **(11)** shows the presence of species $[C_{19}H_{15}N_3O_8]^+$ (413, 100). Complex **(12)** shows $[C_{11}H_{14}N_2O_4Cu]^+$, (301,5, 100) and $[C_{13}H_{26}N_2O_8Cu]^+$ (401,5, 24] and complex **(13)** shows the presence of $[C_{13}H_{10}N_2O_3Co]^+$ (301, 100), $[C_{13}H_3N_2O_4]^+$ (249, 24) and $[C_{11}H_{12}N_3O_3Co]^+$ (293, 26) species. However, complex **(14)** shows the existence of $[C_{11}H_{14}N_2O_3Ni]^+$ (281, 100) and $[C_{13}H_{10}N_2O_3Ni]^+$ (301, 100) species.

Thermal analyses

The thermal behaviour of the complexes **(2)**, **(4)**, **(7)**, **(8)**, **(12)** and **(13)** has been studied using DTA, DTG and TG analyses. Complex **(2)** shows a broad DTA peak at 100°C, which may be assigned to the breaking of H-bonding associated with the lattice or chemical rearrangement of the complex, then two steps of weight loss are observed. The first step at 187 °C, corresponds to the endothermic elimination of two molecules of coordinated water.[31]

The experimental mass loss of 8.1% agrees well with the calculated mass loss of 8.86%. The second step, with an endothermic DTA peak at 240 °C, is due to loss of a coordinated acetate group (Calcd 15.94%. Found 15.30%). Complex **(4)**, shows a broad peak in the DTA curve in the 65–179 °C range, which is due to the elimination of two molecules of hydrated water (Calcd 6.11%. Found 6.57%). Another endothermic peak observed at 370 °C may be assigned to the m.p. of the complex, and the peak at 403 °C is attributed to exothermic loss of ($C_{11}H_{11}N_2O_2$) species (Calcd 37.43%. Found 37.9%). Complex **(7)** undergoes decomposition mainly in four stages. The first stage takes place at 81°C with endothermic loss of CO_2 + hydrated H_2O (Calcd 5.14%. Found 4.84%). The mass loss observed in the second step is due to the loss of another CO_2 (Calcd 3.85%. Found 4.36%). The loss of 2 CO_2 and two molecules of coordinated water occurred at 212 °C (Calcd 14.56%. Found 13.92%). Another endothermic peak at 294 °C, corresponds to the loss of ($C_{11}H_{11}N_2O_2$) species (Calcd 21.62%. Found 22.09%), however, the complex **(8)** shows three-steps of decomposition, the first step at 100 °C, is due to endothermic loss of six hydrated water molecules (Calcd 8.40%. Found 8.06%). The second step takes place at 302 °C and is due to endothermic loss of four coordinated water molecules and two CO_2 molecules (Calcd 13.59%. Found 13.61%). The last step at 448 °C, corresponds to the loss of 4(C_6H_5) species (Calcd 30.28%. Found 30.16%). Complex **(12)** also shows three-steps of decomposition. The first step at 103 °C is due to endothermic loss of one hydrated water molecules (Calcd 4.43%. Found 4,8%). The second step takes place at 206 °C is due to endothermic loss of coordinated H_2O (Calcd 4.64%. Found 5.0%). The last step occurs at 280 °C, corresponds to the loss of coordinated acetate species (Calcd 15.95%. Found 16.23%). Complex **(13)** also shows three steps of decomposition. The first step, which occurs at 155 °C, is due to the loss of three water molecules (Calcd 11.42%. Found 11.91%). The second step takes place at 269 °C and corresponds to loss of three coordinated water molecules (Calcd 12.9%. Found 12.58%). The final step at 354 °C, is due to the loss of one coordinated acetate group (Calcd 16.2%. Found 16.35%).

Biological activity

The antibacterial and antifungal screening data show that the compounds exhibit antibacterial and antifungal properties, which are compared with tetracycline (Bacteria) and Amphotricen B (Fungi). It is important to note that the metal complexes exhibit more inhibitory effects than the parent ligands. It is clear that the zone of inhibition is large for metal complexes against the gram-positive bacteria (*Bacillus subtiles*) and gram-negative bacteria (*Escherichia coli*) compared to tetracyclin as a standard drug. The results of fungicidal screening show that copper(II) complexes **(2),** and **(12),** nickel(II) complexes **(8),** and **(13)** and manganese(II) complexe **(5)** were more highly active than the free ligands against *(Aspergillus Niger)*. The mode of action may involve the formation of a hydrogen bond through the azomethine nitrogen atom, oxygen atom of carboxylic group or oxygen or nitrogen atoms of the oximato group with active centres of the cell constituents, resulting in interference with the normal cell process. The variation in the effectiveness of different compounds against different organisms depends either on the impermeability of the cells of the microbes or the difference in ribosomes of microbial cells. It has also been proposed that the concentration plays a vital role in increasing the degree of inhibition, since as the concentration increases, the activity increases. The increased activity of the metal complexes can be explained on the basis of chelation theory.[52] It is known that the chelation tends to make the ligand act as more powerful and potent bactericidal and fungicidal agents, thus killing more bacteria and fungi than the ligand. It is known that, in a complex, the positive charge of the metal is partially shared with the donor atoms present in the ligands, and there may be π-electron delocalisation over the whole chelating system[53] this increases the lipophilic character of the metal chelate and favours its permeation through the lipoid layer of the membranes. There are other factors which also increase the activity, which are solubility, conductivity, coordination mode and bond length between the metal and the ligand. The order of activity for Gram positive bacteria is **(8)>(2)>(15)>(1) = (6) = (11) = (12) = (13)>(7)** and for Gram negative bacteria is **(2) = (12)>(8)>(5) = (6)>(7) = (11) = (13)>(1) = (15).** However for fungi, the order of activity **(8)>(2)>(12)>(5) = (1)>(13)>(6) = (7) = (15)>(11).**

Received 21 May 2009; accepted 10 August 2009
Paper 090597 doi: 10.3184/030823409X12506792542909

References

1 O. Kahn; *Struct. Bond. (Berlin),* 1987, **68,** 89.
2 G.S. White and D.W. Stephan, *Inorg. Chem.,* 1985, **25,** 1499.
3 W. Plass, *Chemie Unserer Zeit,* 1998, **32,** 323.
4 A. Gleizes, M. Jule, M. Verdaguer, J.A. Real, J. Faus and X. Solans, *J. Chem. Soc., Dalton Trans.,* 1992, 3209.
5 S. Alvarez, M. Julve and M. Verdauger; *Inorg. Chem.,* 1990, **29,** 4501.
6 R. Ruiz. Found Lloret, M. Julve, J. Faus, M.C. Munoz and X. Solans; *Inorg. Chim. Acta,* 1993, **213,** 261.
7 A. Roth, A. Buchholz and W. Plass, *Z. Anorg. Allg. Chem.,* 2007, **633,** 383.
8 D. Plaul, A. Buchholz, H. Görls and W. Plass, *Polyhedron,* 2007, **26,** 4581.
9 W. Huang, P. Yang Sun, J. Linfang, Y. Feisun and S. Hua Gou, *Trans. Met. Chem.,* 2003, **28,** 925.
10 A. Zharkouskaya, H. Görls, G. Vaughan and W. Plass, *Inorg. Chem. Comm.,* 2005, **8,** 1145.
11 A. Zharkouskaya, A. Buchholz and W. Plass, *Eur. J. Inorg. Chem.,* 2005, 4875.
12 M.M. Aly and A.M. El-Awad, *J. Inorg. Nucl. Chem.,* 1980, **42,** 1295.
13 M.M. Aly, *Inorg. Nucl. Chem. Lett.,* 1979, **15**, 17.
14 M.M. Aly and N.I. Al-Shatti, *Trans. Met. Chem.,* 1998, **23,** 361.
15 H.A. El-Boraey and A.S. El-Tabl, *Polish J. Chem.,* 2003, **77,** 1759.
16 K.C. Pande, *U. S. Patent;* 1966, **3,** 252, 672; *Chem. Abstr.,* 1967, **66,** 28, 8910.
17 R.J. Banner, A.J. Charlson, R.P. Gale, K.E. Traimer and E.C. Wattom, *Metal in medicine Conference Abstr.,* University of Sydney, 1975, p. 12.
18 F.J. Welcher, *Organic analytical reagents*, Van Nostrand, New York, 1955, P. 280.
19 R.F.F. Costa, A.P. Rebolledo, T. Metencio, *J. Coord. Chem.,* 2005, **58,** 1307.
20 A. Bilgin, K. Serbest and Y. Gök, *Trans. Met. Chem.,* 2002, **25,** 63.
21 G. Tircso, A. Benyei, E. Brucher, A. Kis and R. Kiraly, *Inorg. Chem.,* 2006, **45,** 4951.
22 N. Raman, A. Kulandasamy, C. Thangaraja, P. Manisankar, S. Viswanathan and C. Vedhi, *Trans. Met. Chem.,* 2004, **29**, 129.
23 A.S. El-Tabl, *Trans. Met. Chem.,* 2002, **27,** 166.
24 A. Kilic, E. Tas, B. Gumgum and I. Yilmaz, *Trans. Met. Chem.,* 2006, **31,** 46.
25 A.S. El-Tabl. FoundA. El-Saied and A.N. Al-Hakimi, *Trans. Met. Chem.,* 2007, **32,** 689.
26 S.A. Sallam, *Trans. Met. Chem.,* 2006, **31,** 46.
27 A.S. El-Tabl, *Trans. Met. Chem.,* 1997, **22,** 400.
28 Y.B. Jian, H.Z. Kou, R.J. Wang and J. Ribas, *Inorg. Chem.,* 2005, **44,** 709.
29 B. Sreenivasulu. Found Zhao, S. Gao and J.J. Vittal, *Eur. J. Inorg. Chem.,* 2006, 2656.
30 K. Nakamoto, *The infrared and raman spectra of inorganic and coordination compounds,* 3rd edn, Wiley, New York, 1978.
31 A.S. El-Tabl, *J. Chem. Res.* (S), 2002, 529*, J. Chem. Res.* (M), 2002, 1110.
32 W.J. Geary, *Coord. Chem. Rev.,* 1971, **7,** 81.
33 C. Fraser and B. Bosnich, *Inorg. Chem.,* 1994, **33,** 338.
34 A.S. El-Tabl, *Polish J. Chem.,* 1997, **71,** 1213.
35 A.S. El-Tabl and S.M. Imam, *Trans. Met. Chem.,* 1997, **22,** 259.
36 N.V. Thakkar and S.Z. Bootwala, *Indian J. Chem.,* 1995, **34A,** 370.
37 S.A. Sallam, A.S. Arabi, B.A. El-Shetary and A. Lentz, *Trans. Met. Chem.,* 2002, **27,** 447.
38 S. Chandra and S. Sharma, *Trans. Met. Chem.,* 2002, **27,** 732.
39 S. Chandra and U. Kumar, *Spectrochim. Acta, Part A,* 2005, **61,** 219.
40 A.B P. Lever, *Inorganic electronic spectroscopy*, 2nd Ed., Elsevier, Amsterdam, 1984.
41 A. El-Motaleb and M Gaber, *Trans. Met. Chem.,* 1997, **22,** 211.
42 R.A. Lal and A. Kumar, *Indian J. Chem.,* 1999, **38A,** 839.
43 J.K. Nag, S. Pal and C. Sinha, *Trans. Met. Chem.,* 2005, **30,** 523.
44 N. Raman, Y. Pitchaikani and A. Kulandaisamy, *Proc. Indian Aca. Sci. (Chem. Sc.),* 2001, **133** 183.
45 K.B. Gudasi, S.A. Patil, R.S. Vadvavi, R.V. Shenoy and M. Nethaji, *Trans. Met. Chem.,* 2006, **31,** 586.
46 A.S. El-Tabl, *Trans. Met. Chem.,* 1998, **23,** 63.
47 A.S. El-Tabl, *Bull. Korean Chem. Soc.,* 2004, **25,** 1757.
48 A.S. El-Tabl, PhD Thesis, Faculty of Science, Menoufia University, Egypt (1993).
49 A.S. El-Tabl. Found A. El-Saied, W. Plass and A.N. Al-Hakimi, *Spectrochim. Acta, Part A,* 2008, **71,** 90.
50 A.S. El-Tabl and R.M. Issa, *J. Coord. Chem.,* 2004, **57,** 509.
51 R.K. Kay and G.B. Kauffman, *Inorg. Chim. Acta,* 1990, **174,** 257; 1990,**174,** 237.
52 Z.H.A. El-Wahab, M.M. Mashaly, A.A. Salman, B.A. El-Shetary and A.A. Fahei, *Spectrochim. Acta Part A,* 2004, **60,** 2861.
53 S.K. Sengupta, O.P. Pandey, B.K. Srivastava and V.K. Sharma, *Trans. Met. Chem.,* 1998, **23**, 349.